

Nonlinear conductance of long quantum wires at a conductance plateau transition: Where does the voltage drop?

T. Micklitz¹, A. Levchenko², and A. Rosch³

¹*Dahlem Center for Complex Quantum Systems and Institut für Theoretische Physik,
Freie Universität Berlin, 14195 Berlin, Germany*

²*Department of Physics and Astronomy, Michigan State University, East Lansing, MI 48824, USA*

³*Institut für Theoretische Physik, Universität zu Köln, Zùlpicher Str. 77, 50937 Cologne, Germany*

(Dated: February 19, 2012)

We calculate the linear and nonlinear conductance of spinless fermions in clean, long quantum wires where short-ranged interactions lead locally to equilibration. Close to the quantum phase transition where the conductance jumps from zero to one conductance quantum, the conductance obtains an universal form governed by the ratios of temperature, bias voltage and gate voltage. Asymptotic analytic results are compared to solutions of a Boltzmann equation which includes the effects of three-particle scattering. Surprisingly, we find that for long wires the voltage predominantly drops close to one end of the quantum wire due to a thermoelectric effect.

PACS numbers: 71.10.Pm, 72.10.-d, 72.15.Lh

Introduction.— A clean quantum wire with adiabatic contacts is characterized by a quantized conductance, $G = nG_0$ with $G_0 = e^2/h$. The integer n describes the number of conduction channels (including spin). The conductance quantization is closely related to charge quantization and survives (for sufficiently low temperatures T) even in the presence of interactions [1–3] as long as momentum relaxation by Umklapp scattering can be neglected [4, 5].

The transition from one conductance plateau to the next is an example of a quantum phase transition without order parameter, where only a topological property, the number of conducting channels, changes. While the thermodynamics of this quantum critical point (QCP) is quite well understood [6–9], a theory of the quantum critical conductance is much more challenging: How does the conductance change from one conductance plateau to the next at low but finite T ? We will answer this question both in the linear and non-linear regime for the most simple situation, i.e., the transition from $n = 0$ to $n = 1$ for spinless fermions with finite-ranged interactions. Here the QCP describes the transition from zero to a finite fermion density. As interactions are irrelevant at this QCP, thermodynamic properties are well described by non-interaction fermions [5, 10] but transport in long wires is still governed by collisions. Relaxation by collisions and non-equilibrium dynamics in one-dimensional (1D) systems have recently moved into the focus of theoretical [11–18] and experimental [19–21] research.

A general question is where the voltage drops when a finite current is driven through a clean 1D quantum wire by applying a bias voltage V . For diffusive (multichannel) quantum wires one expects a linear drop of the voltage (i.e. of the electrochemical potential) across the wire while for non-interacting, ballistic quantum wires the voltage drop occurs only close to the two contacts [22]. In clean *interacting* quantum wires with low fermion den-

sity (and therefore negligible Umklapp scattering) the dc conductivity is infinite for an infinitely long wire due to momentum conservation, $\sigma(T) = \infty$. The vanishing resistivity strongly suggests that there is again no voltage drop inside the wire.

A recent series of papers [23–27], which studied the role of equilibration in long but finite quantum wires of length L , found that in the linear response regime, $V \rightarrow 0$, there is a linear drop of voltage [25] along the wire. We resolve this apparent contradiction to $\sigma(T) = \infty$ by noting that the limits $V \rightarrow 0$ and $L \rightarrow \infty$ do not commute. The drop of voltage is governed by a new length scale ℓ_V which diverges for $V \rightarrow 0$. For $L \ll \ell_V$ a linear drop of voltage occurs. In the opposite limit, $L \gg \ell_V$, however, the voltage drops only within a distance of ℓ_V of the contacts. Surprisingly, the voltage drop is not symmetrical and occurs predominantly only at one of the two contacts!

Previous work on equilibrated quantum wires [23–27] focused on the limit $T \ll \epsilon_F$, where ϵ_F is the Fermi energy. As scattering processes equilibrating left-moving and right-moving fermions involve the bottom of the band [18, 25–28], they are exponentially suppressed and therefore the corresponding equilibration length is exponentially large, $\ell_{\text{eq}} \sim e^{\Delta/T}$, where $\Delta \approx \epsilon_F$ for weak interactions (thermal equilibration relevant for heat conduction occurs on shorter length scales [29]). For $L \gg \ell_{\text{eq}}$ it was found that the quantized (linear) conductance obtains corrections of order $(T/\Delta)^2$. Large effects can therefore be expected close to the conductance plateau transition, where $\Delta \sim T$, as studied in this paper.

Model.— We consider 1D spin-polarized electrons with quadratic dispersion $\epsilon_p = \frac{p^2}{2m}$, interacting via a short range potential. Close to the QCP, where filling of the first subband becomes small, interactions are strongly irrelevant in the renormalization group sense [6, 30] and a single electron description becomes approximately valid. To study equilibration and its effect on transport we may

thus use the Boltzmann equation

$$v_p \partial_x f_{x,p} = -I_{x,p}^{\text{col}}[f], \quad (1)$$

where $f_{x,p}$ is the quasiclassical distribution function, $v_p = p/m$ the velocity, and the collision integral I^{col} describes collisions. The contacts of the quantum wire to the leads at $x = \pm \frac{L}{2}$ induce boundary conditions for electrons moving *into* the quantum wire

$$f_{x=-\frac{L}{2}, p>0} = \frac{1}{e^{\xi_p^l/T} + 1}, \quad f_{x=\frac{L}{2}, p<0} = \frac{1}{e^{\xi_p^r/T} + 1}, \quad (2)$$

where $\xi_p^{l/r} = \epsilon_p - \mu \mp eV/2$ with $\mu = 0$ at the QCP. Here we assume adiabatic and ballistic contacts, i.e., contacts which are smooth compared to the electronic wavelength but short in comparison to the scattering length.

In 1D systems energy and momentum conservation severely restrict the phase space available for scattering: in a two-particle process, two particles of equal mass can only exchange their momenta [6, 18] which leaves f_p unchanged. One therefore has to study the effects of three particle collisions [18, 28] described by

$$I_{x,p_1}^{\text{col}}[f] = \sum_{\substack{p_2 p_3 \\ p'_1 p'_2 p'_3}} W_{123}^{1'2'3'} [f_1 f_2 f_3 (1-f_{1'}) (1-f_{2'}) (1-f_{3'}) - f_{1'} f_{2'} f_{3'} (1-f_1) (1-f_2) (1-f_3)] \quad (3)$$

where the scattering rate $W_{123}^{1'2'3'}$ arises to fourth order in the bare two-particle interactions [31]. For low energies and spinless fermions, Pauli principle ensures that it takes the universal form

$$W_{123}^{1'2'3'} = W((p_1 - p_2)(p_1 - p_3)(p_2 - p_3) (p'_1 - p'_2)(p'_1 - p'_3)(p'_2 - p'_3))^2 \delta_{P_i, P_f} \delta(E_i - E_f) \quad (4)$$

where $P_{i(f)} = p_1 + p_2 + p_3$ and $E_{i(f)} = \epsilon_1 + \epsilon_2 + \epsilon_3$ are the total momentum and energy of the three scattering particles before (after) the collision, respectively. A simple dimensional analysis allows to identify a characteristic length scale of equilibration at the QCP ($\mu = 0$) by setting typical momenta to $\sqrt{2mT}$

$$\frac{1}{\ell_{\text{eq}}} = \frac{2Wm^2 L^4}{(2\pi\hbar)^4} (2mT)^{13/2} \quad (5)$$

Measuring all length scales in units of ℓ_{eq} and all momenta in units of $\sqrt{2mT}$ allows to scale out the parameters W , m and T and the only remaining parameters are L/ℓ_{eq} , eV/T and μ/T . We have checked both numerically and analytically that close to the QCP Hartree-Fock potentials (not included in Eq. (1)) can be neglected.

For a numerical solution of the Boltzmann equation (1) it is important to avoid discretization errors leading to a violation of conservation laws. We therefore use a conservative splitting method following Ref. [32], see supplement [30], to solve the time-dependent Boltzmann equation until a steady state has been reached. For the linear

response calculation we use a linearized collision integral.

Conservation laws.— Three conservation laws govern transport in long quantum wires: charge, energy and momentum conservation. The corresponding currents are the charge current, $j_c = e \sum_p v_p f_p$, the energy current, $j_E \approx \sum_p \epsilon_p v_p f_p$, and the momentum current, $j_p \approx \sum_p p v_p f_p$. The latter can be identified with pressure. For sufficiently long quantum wires and far away from the contacts the system will reach locally equilibrium with the distribution function

$$f_p^{\text{eq}}(u, \mu, T) = [1 + e^{\frac{(p-mu)^2}{2mT} - \frac{\mu}{T}}]^{-1} \quad (6)$$

parametrized by three space-dependent Lagrange parameters $\mu(x)$, $T(x)$ and the velocity $u(x)$ reflecting the three conservation laws. For the distribution function (6) one can calculate the corresponding equilibrium currents j_c^{eq} , j_E^{eq} and j_p^{eq} as function of μ , T and u .

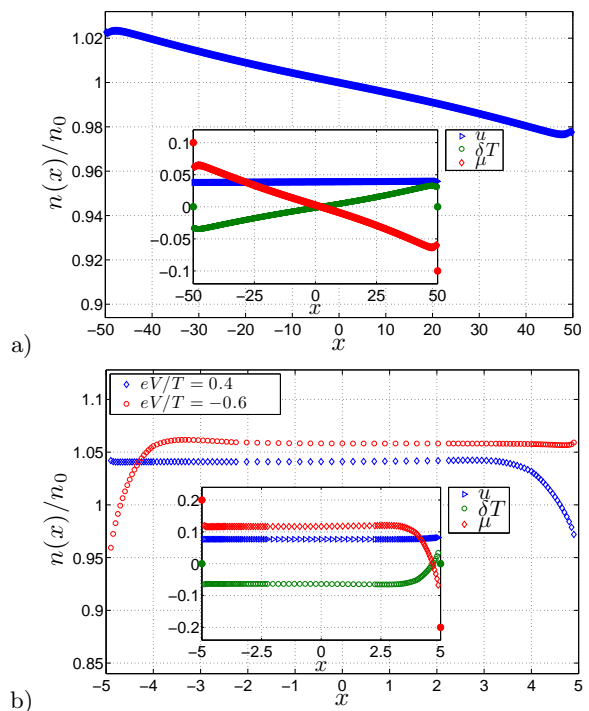


FIG. 1: (Color online) Electron density, $n(x) = n_0(1 + \delta n(x))$, at the QCP ($\mu = 0$) calculated from a solution of the Boltzmann equation (1), using (a) a linearized collision integral for $L = 100\ell_{\text{eq}}$ and $V \rightarrow 0$ and (b) the non-linearized collision integral for $L = 10\ell_{\text{eq}}$ and larger voltages, $eV/T = 0.4$ and $eV/T = -0.6$ (inset: $eV/T = 0.4$). The inset shows $\mu(x)$, $\delta T(x) = T(x) - T$ and $u(x)$ (in units of T and $\sqrt{2T/m}$) obtained from fitting the local charge, energy and momentum densities to Eq. (6). While in the linear response regime, $L \ll |\ell_V|$, there is a linear voltage drop across the wire, the voltage (and the density) drops predominantly close to one of the two contacts for $L \gg |\ell_V|$. Note that due to a finite drift u the chemical potentials close to the contacts do not match the chemical potential $\mu \pm eV/2$ in the leads (shown as separate dots at $x = \pm L/2$ in the insets).

Voltage drop.— Fig. 1 shows the density profile and the local chemical potential (insets) of long quantum wires, $L \gg \ell_{\text{eq}}$, obtained from our Boltzmann simulations (the supplement [30] discusses how $\mu(x)$ and $T(x)$ can be measured by tunneling contacts). For small V (Fig. 1a) there is both a linear drop of the chemical potential along the wire and a finite jump directly at the two contacts (the separate points at $x = \pm L/2$ show μ in the leads). In an experiment, this jump will occur on the length scale describing the crossover from the 1D lead to the higher-dimensional contacts. This jump is also present for larger V (Fig. 1b), where, however, the linear voltage drop is absent. Surprisingly, there is instead a large *asymmetric* voltage drop which occurs only close to one of the two contacts. This behavior occurs for sufficiently long wires not only directly at the QCP but also away from it. Interestingly, one observes cooling instead of heating close to the left contact. Though unexpected at first glance, it can be related [25] to the finite boost u in (6), which is partially compensated by a reduced temperature to match the boundary condition for right-movers.

The qualitative difference between small and larger voltage can be understood from a simple argument based on matching currents. The steady state for $V > 0$ is characterized by the three currents j_c , j_E and j_p . From the three equations $j_\alpha = j_\alpha^{\text{eq}}$, $\alpha = c, E, p$, one can, for sufficiently long wires, determine the three parameters μ , T and u which will be constant along the wire as $j_\alpha = \text{const.}$. Therefore, for a sufficiently long wire and finite V , a voltage drop can occur only close to the contacts. In the linear response regime, i.e. for small V , the situation is, however, different. By setting only one of the three parameters, u , to zero, two currents, j_c^{eq} and j_E^{eq} , vanish in equilibrium. As both j_c^{eq} and j_E^{eq} are linear in u , their ratio $j_c^{\text{eq}}/j_E^{\text{eq}}$ is – in the limit of small V – fixed by the average μ and T . This is used below when calculating the linear-response conductance analytically.

To develop an approximate analytical theory valid in both regimes, we consider small, but finite voltages V and parametrize $f_{x,p}$ by

$$f_{x,p} = f_{x,p}^{\text{eq}} + \delta f_{x,p}, \quad (7)$$

where $\delta f_{x,p}$ accounts for deviations from local equilibrium $f_{x,p}^{\text{eq}} = f_p^{\text{eq}}(u(x), \mu(x), T(x))$. Here it is convenient to determine $\mu(x)$, $T(x)$ and $u(x)$ from the two equations $j_c = j_c^{\text{eq}}$ and $j_p = j_p^{\text{eq}}$ while the third parameter is fixed by fitting the local density $n(x) = n^{\text{eq}}(x)$.

By linearizing the Boltzmann equation (1) in δf , one obtains that δf is proportional to $\partial n / \partial x$. For the energy current, one therefore obtains

$$j_E = j_E^{\text{eq}} + \tilde{D} \frac{\partial n}{\partial x} = \text{const.} \quad (8)$$

where \tilde{D} is the thermoelectric diffusion constant describing how density gradients generate energy currents. Us-

ing Kubo's formula and Einstein relations, \tilde{D} can be calculated from the product of a correlation function of the heat- and particle current and the compressibility.

For small voltages \tilde{D} is approximately constant across the wire. Using Galilei invariance which implies $u = j_c^{\text{eq}} / en^{\text{eq}} = j_c / en$, we obtain $j_E^{\text{eq}} = \frac{3j_p j_c}{2en} - \frac{m j_c^3}{e^3 n^2}$. For small V the last term can be neglected and one can linearize the density $n = n_0 + \delta n$ to obtain

$$-\frac{3j_p j_c}{2en_0^2} \delta n + \tilde{D} \frac{\partial \delta n}{\partial x} \approx j_E - \frac{3j_p j_c}{2en_0} = \text{const.} \quad (9)$$

This equation introduces a new length scale

$$\ell_V = \frac{2\tilde{D}en_0^2}{3j_p j_c} \quad (10)$$

which diverges for $V \rightarrow 0$ as j_c vanishes in this limit while \tilde{D} , n_0 and j_p remain finite. For $|eV| \ll T$ and $\mu = 0$, i.e., at the QCP, a simple dimensional analysis gives $\ell_V \sim \ell_{\text{eq}} \frac{T}{eV}$.

For $L \ll |\ell_V|$, one obtains from Eq. (9) $\frac{\partial \delta n}{\partial x} = \text{const.}$ and therefore a linear drop in density and local chemical potential as in our numerical results, Fig. 1a. In the other limit, $L \gg |\ell_V|$, δn obtains an exponential x dependence

$$n(x) = n_L + (n_R - n_L) \exp\left[\frac{x - L/2}{\ell_V}\right] \quad (11)$$

with $n_{L/R} \approx n(\mp L/2)$. The direction of the current determines whether the drop of density and voltage occur at the right ($\ell_V > 0$) or left ($\ell_V < 0$) lead, see Fig. 1b. This shows that the strongly asymmetric drop of voltage arises from a thermoelectric effect captured by the simple hydrodynamic equation (9).

Linear response regime.— Interestingly, it is possible to calculate in the linear response regime the quantum critical conductance for long quantum wires ($\ell_{\text{eq}} \ll L \ll |\ell_V|$) analytically. We use the approach developed in Ref. [23, 25] (where only $T \ll \mu$ was considered) and keep track of the change of the charge and energy current carried by *right-moving* electrons with $p > 0$, $j_c^R(x) = e \sum_{p>0} v_p f_{x,p}$ and $j_E^R(x) = \sum_{p>0} v_p \epsilon_p f_{x,p}$, respectively. We use that far away from the contacts the distribution function obtains local equilibrium, $f_{x,p} \approx f_{x,p}^{\text{eq}}$, described by Eq. (6) with $T(x) = T + \delta T(x)$, $\mu(x) = \mu + \delta \mu(x)$ and $u(x)$. This allows to calculate directly j_c , j_c^R , j_E , j_E^R and j_p in terms of three unknown functions, $u(x)$, $\delta \mu(x)$ and $\delta T(x)$. Current conservation implies $u(x) = \text{const.}$ Furthermore, the ratio $r_1 = j_E / j_c$ is to linear order just a simple function of μ and T independent of V and u . The condition of constant momentum current fixes another ratio, $r_2 = \partial_x \delta T / \partial_x \delta \mu$. This result is used to eliminate all unknowns from the ratio $r_3 = \partial_x j_E^R / \partial_x j_c^R$. To leading order, r_1 , r_2 and r_3 are space independent functions of μ and T (calculated in the supplementary material [30]). Finally, one identifies [23] the difference in the charge

(energy) current of the interacting- and non-interaction system as the total change in the right-moving charge (energy) current along the wire, $j_c = j_c^0 + \int \partial_x j_c^R dx$ ($j_E = j_E^0 + \int \partial_x j_E^R dx$), respectively. If we now assume (as we checked numerically), that these integrals are dominated by their bulk contribution, we obtain the equation

$$r_3 = \frac{r_1 j_c - j_E^0}{j_c - j_c^0} \quad (12)$$

from which one can calculate directly j_c . Combining all results [30], we find for the linear-response conductance up to corrections of $\mathcal{O}(\ell_{\text{eq}}/L)$, i.e. for $\ell_{\text{eq}} \ll L \ll |\ell_V|$

$$G(z) = \frac{e^2}{h} \frac{\alpha_0(z)\alpha_2(z) - \alpha_1^2(z)}{\alpha_2(z) + \alpha_0(z)\kappa^2(z) - 2\alpha_1(z)\kappa(z)}, \quad (13)$$

where $z = \mu/T$, $\langle \dots \rangle_z = -\int_{-z}^{\infty} d\xi \langle \dots \rangle \frac{df_\xi^0}{d\xi}$, with $f_\xi^0 = \frac{1}{1+e^\xi}$ and $\alpha_k = \langle \xi^k \rangle_z$, $\kappa = \frac{\langle \xi \sqrt{z+\xi} \rangle_z}{\langle \sqrt{z+\xi} \rangle_z}$. At the QCP, i.e., for $\mu = 0$, this gives

$$\frac{G_{\text{QCP}}}{e^2/h} = \frac{\frac{\pi^2}{6} - 2 \ln^2 2}{\frac{\pi^2}{3} + \frac{9}{8} \frac{\zeta^2(3/2)}{\zeta^2(1/2)} + \frac{6}{\sqrt{2}} \frac{\zeta(3/2)}{\zeta(1/2)} \ln 2} \approx 0.420 \quad (14)$$

with $\zeta(x)$ the Riemann zeta function. G_{QCP} is about 16% below the non-interacting result $e^2/2h$.

Fig. 2 displays the linear response conductance as functions of μ/T for non-interacting (see below) and fully equilibrated electrons which have a clearly different shape. Our analytical formula (13) fits very well the numerical result (symbols).

Shorter wires.— Upon lowering T , ℓ_{eq} rapidly increases, see Eq. (5). For quantum wires, where $L/\ell_{\text{eq}} \ll 1$, one can neglect the effects of equilibrating interactions.

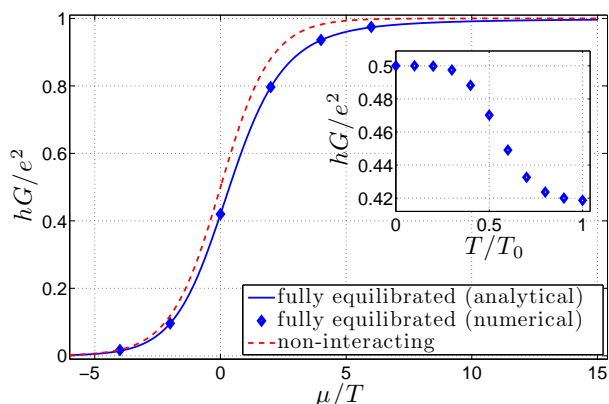


FIG. 2: (Color online) Conductance of fully equilibrated (solid line) and non-interacting electrons (dashed line) in the linear response regime ($\ell_{\text{eq}} \ll L \ll |\ell_V|$). Numerical results (symbols) agree with Eq. (13). Inset: Upon lowering T , ℓ_{eq} grows rapidly and a crossover from the equilibrated to the non-interacting conductance is observed for $\ell_{\text{eq}} \sim L$ ($L = 10\ell_{\text{eq}}, \mu = 0$).

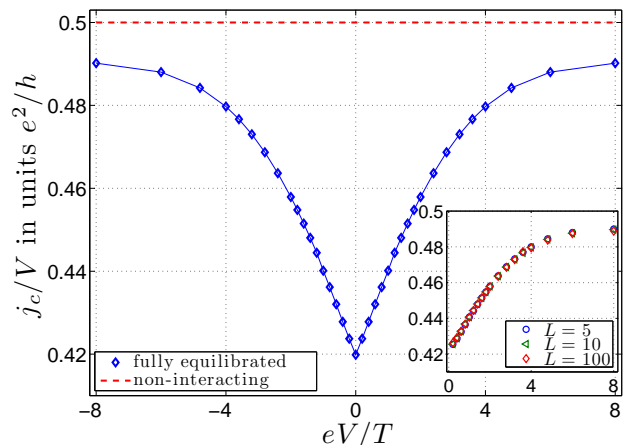


FIG. 3: (Color online) Non-linear conductance, j_c/V obtained for $L = 7.5\ell_{\text{eq}}$ from a numerical solution of the Boltzmann equation. For $eV/T \rightarrow 0$ a linearized collision integral was used. Inset: Within our numerical precision, there is no finite size dependence of the non-linear conductance for $L \gg \ell_{\text{eq}}$ (L measured in units ℓ_{eq}).

Half of the voltage drops at the left and right contact, respectively, and there is no voltage drop inside the wire as $f_{x,p} = f_p$ is independent of x . For j_c one obtains the well-known non-interacting result $j_c^0 = \frac{eT}{h} \ln \left[\frac{1+e^{(\mu+eV/2)/T}}{1+e^{(\mu-eV/2)/T}} \right]$. The conductance plateau transition in linear response is therefore described by $G(\mu/T) = G_0/(1 + e^{-\mu/T})$ while at $\mu = 0$ the current is for arbitrary eV/T given by $j_0 = G_0V/2$. In the inset of Fig. 2 we have calculated numerically the crossover from the interacting quantum critical conductance (14) to the non-interacting one, which occurs upon lowering T when $\ell_{\text{eq}} \sim L$.

Nonlinear response.— Fig. 3 show the nonlinear conductance j_c/V at the QCP, i.e. for $\mu = 0$. It interpolates between the linear-response value (14) and the non-interacting result obtained for $|eV|/T \rightarrow \infty$. For $|eV| \gg T$ and $\mu = 0$ all states with $p > 0$ and $\epsilon_p < |eV|/2$ are occupied. As this is also an equilibrium distribution function with $u = \sqrt{|eV|/4m}$ and $\mu = mu^2/2$, collisions have no effects in this limit.

For small V the nonlinear conductance appears to be non-analytic,

$$j_c(V) = G_{\text{QCP}}V + \gamma|V|V + \dots \quad (15)$$

which can be traced back to the asymmetric voltage drop for $L \gg |\ell_V|$. As $n_R - n_L$ in Eq. (11) varies linear in V , the density in the center, $n(0) \approx \max(n_R, n_L)$ according to Eq. (11), obtains for $L \gg |\ell_V|$ a correction proportional to $|V|$. As $j_c \approx eun$, this implies a correction proportional to $|V|V$ to the current as soon as $L \gg |\ell_V|$. Due to numerical problems, we were not able to obtain reliable numerical results in the small- V regime $L \lesssim |\ell_V|$ where we expect a rounding of the non-analytic correction. Overall, the finite size corrections to the non-linear

conductance are smaller than our numerical resolution for $L \gg \ell_{\text{eq}}$, see inset of Fig. 3.

Outlook.— While our results have been derived only for spinless fermions with short ranged interactions, we expect that our main qualitative results are also of direct relevance for quantum wires made of electrons with spin and long-ranged Coulomb interactions. For these systems, the hydrodynamic equation (9) should also be valid (with strongly modified parameters) at least if gates provide screening. The highly asymmetric voltage drop predicted by us will probably be even much easier to observe, as the stronger interactions imply that the regimes $L \gg \ell_{\text{eq}}$ and $L \gg |\ell_V|$ are much easier to reach. In recent experiments with ultracold atoms [33] an atomic current was driven through a long quantum channel connecting two reservoirs and the resulting density profile (and therefore the drop of the chemical potential) was directly measured. This opens new exciting possibilities to verify our predictions also in cold-atom experiments.

We would like to thank E. Sela, M. Garst, G. Zarand and especially J. Rech and K. A. Matveev for useful discussions and acknowledge financial support by the DFG (SFB 608, FOR 960).

-
- [1] D. L. Maslov and M. Stone, Phys. Rev. B **52**, R5539 (1995).
- [2] V. V. Ponomarenko, Phys. Rev. B **52**, R8666 (1995).
- [3] I. Safi and H. J. Schulz, Phys. Rev. B **52**, R17040 (1995).
- [4] A. Rosch and N. Andrei, Phys. Rev. Lett. **85**, 1092 (2000).
- [5] T. Giamarchi, *Quantum Physics in One Dimension*, (Oxford University Press, 2004).
- [6] Subir Sachdev, *Quantum Phase Transitions*, (Cambridge University Press, 2000).
- [7] L. Balents, Phys. Rev. B **61**, 4429 (2000).
- [8] T. Meng, M. Dixit, M. Garst, J. S. Meyer, Phys. Rev. A **83**, 125323 (2011).
- [9] M. Sitte, A. Rosch, J. S. Meyer, K. A. Matveev, M. Garst, Phys. Rev. Lett. **102**, 176404 (2009).
- [10] T. Lorenz, O. Heyer, M. Garst, F. Anfuso, A. Rosch, Ch. Ruegg, K. Kramer, Phys. Rev. Lett. **100**, 067208 (2008).
- [11] S. N. Dinh, D. A. Bagrets, A. D. Mirlin, Phys. Rev. B **81**, 081306 (R) (2010).
- [12] D. B. Gutman, Y. Gefen, and A. D. Mirlin, Phys. Rev. Lett. **101**, 126802 (2008).
- [13] D. B. Gutman, Y. Gefen, and A. D. Mirlin, Phys. Rev. B **81**, 085436 (2010).
- [14] S. Takei, M. Milletter, and B. Rosenow, Phys. Rev. B **82**, 041306 (2010).
- [15] T. Karzig, L. I. Glazman, F. von Oppen, Phys. Rev. Lett. **105**, 226407 (2010).
- [16] A. Imambekov, L. I. Glazman, Science **323**, 228 (2009).
- [17] M. Khodas, M. Pustilnik, A. Kamenev, and L. I. Glazman, Phys. Rev. B **76**, 155402 (2007).
- [18] A. M. Lunde, K. Flensberg, and L. I. Glazman, Phys. Rev. B **75**, 245418 (2007).
- [19] C. Altimiras, H. le Sueur, U. Gennser, A. Cavanna, D. Maily, and F. Pierre, Nature Phys. **6**, 34 (2009).
- [20] Y. F. Chen, T. Dirks, G. Al-Zoubi, N. O. Birge, and N. Mason, Phys. Rev. Lett. **102**, 036804 (2009).
- [21] G. Barak, H. Steinberg, L. N. Pfeiffer, K. W. West, L. I. Glazman, F. von Oppen, and A. Yakoby, Nature Phys. **6**, 489 (2010).
- [22] Y. Imry, *Introduction to mesoscopic physics*, (Oxford, 1997).
- [23] J. Rech, T. Micklitz, and K. A. Matveev, Phys. Rev. Lett. **102**, 116402 (2009).
- [24] K. A. Matveev, A. V. Andreev, Phys. Rev. Lett. **107**, 056402 (2011).
- [25] T. Micklitz, J. Rech, and K. A. Matveev, Phys. Rev. B **81**, 115313 (2010).
- [26] K. A. Matveev, A. V. Andreev, arXiv:1107.4116.
- [27] K. A. Matveev, A. V. Andreev, M. Pustilnik, Phys. Rev. Lett. **105**, 046401 (2010).
- [28] A. Levchenko, Z. Ristivojevic, and T. Micklitz, Phys. Rev. B **83**, 041303 (2011).
- [29] A. Levchenko, T. Micklitz, Z. Ristivojevic, K. A. Matveev, Phys. Rev. B **84**, 115447 (2011).
- [30] See supplementary material.
- [31] For a short-ranged interaction potential $V(x) = V_0 e^{-q_0|x|/\hbar}$ we find $W = \frac{2\pi}{\hbar} \left(\frac{9m\hbar^2}{2\pi^2 L^2} \frac{V_0^2}{q_0^2} \right)^2$.
- [32] V. V. Aristov, *Direct Methods for Solving the Boltzmann Equation and Study of Nonequilibrium Flows*, (Kluwer, 2001).
- [33] J.-P. Brantut, J. Meineke, D. Stadler, S. Krinner, and T. Esslinger, arXiv:1203.1927v2 (2012).

Supplementary material to: “Nonlinear conductance of long quantum wires at a conductance plateau transition: Where does the voltage drop?”

T. Micklitz¹, A. Levchenko², and A. Rosch³

¹*Dahlem Center for Complex Quantum Systems and Institut für Theoretische Physik, Freie Universität Berlin, 14195 Berlin, Germany*

²*Department of Physics and Astronomy, Michigan State University, East Lansing, MI 48824, USA*

³*Institut für Theoretische Physik, Universität zu Köln, Zùlpicher Str. 77, 50937 Cologne, Germany*

(Dated: February 19, 2012)

In this supplementary material we discuss (i) the irrelevance of short range interaction for spinless fermions, (ii) our numerical implementation of the Boltzmann equation, (iii) some more details on the calculation of the linear-response conductance and, finally, (iv) how a voltage drop along the quantum wire can be measured.

PACS numbers: 71.10.Pm, 72.10.-d, 72.15.Lh

Irrelevance of short ranged interactions at QCP

The imaginary-time action describing spinless fermion with short ranged interaction at the QCP ($\mu = 0$) takes the form

$$S = \int d\tau \int dx \left\{ \bar{\psi} \left(\partial_\tau - \frac{\hbar^2}{2m} \partial_x^2 \right) \psi + V \bar{\psi} (\partial_x \bar{\psi}) (\partial_x \psi) \psi \right\} \quad (\text{S16})$$

The derivatives in the interaction term reflect Pauli’s principle, $\psi^2 = 0$. From this action one can directly read off the scaling dimensions of the field, $[\psi] \sim L^{-1/2}$, and the (imaginary) time, $[\tau] \sim L^2$, for $[x] \sim L$. This simple power-counting shows that the interaction strength scales to smaller values, $V \rightarrow V/\lambda$, as the distance of Fermions is increased, $x \rightarrow \lambda x$, or as temperature is lowered, $T \rightarrow T/\lambda^2$. Therefore the interactions are irrelevant at the QCP. This result also implies that the quasiparticle picture and therefore the Boltzmann equation becomes asymptotically exact upon approaching the QCP.

Conservative splitting method

For the numerical implementation of the Boltzmann equation we follow Ref. [3] and solve the time-dependent Boltzmann equation, by splitting time evolution into a free flow and a relaxation stage. The advantage of the splitting procedure is that the distribution obtained after a relaxation step can be corrected such that conservation laws are fulfilled in each collision, see Ref. [3] for details.

Free flow and relaxation steps were implemented by a finite difference scheme, i.e. by discretizing two-dimensional phase-space. We used a first order implicit-explicit upwind scheme to model the free propagation step, and an implicit scheme for the relaxation step [3]. The steady state is reached when currents of the conserved quantities, j_c , j_p and j_E are constant along the wire. For the linear response calculation we parametrize $f_{x,p} = f_p^0 + \delta f_{x,p}$, where f_p^0 is the distribution at zero bias

and $\delta f_{x,p}$ is linear in V , and linearize the collision integral in δf . For the numerically more demanding calculations employing the full collision integral we used meshes with 22 and 42 points in momentum space and various different homogeneous and inhomogeneous discretization of space with ~ 100 grid-points. We checked that our results are independent of discretization.

Linear conductance in long wires

A method to calculate the linear conductance in long wires $\ell_{\text{eq}} \ll L \ll |\ell_V|$, based on conservation laws and the distribution of fully equilibrated electrons Eq. (6) in the main text, was originally introduced in Refs. [1, 2]. As described in the main text, we need to calculate the ratios $r_1 = j_E/j_c$, $r_2 = \partial_x \delta T / \partial_x \delta \mu$ and $r_3 = \partial_x j_E^R / \partial_x j_c^R$. The current j_c in response to the applied voltage (to linear order V) is then found from

$$r_3 = \frac{r_1 j_c - j_E^0}{j_c - j_c^0} \quad (\text{S17})$$

where j_c^0 and j_E^0 are the (linear response) charge and energy currents of non-interacting electrons which is directly described by Eq. (2) of the main text,

$$j_c^0 = \frac{e^2 V}{h} \alpha_0, \quad j_E^0 = \frac{eV}{h} (\mu \alpha_0 + T \alpha_1), \quad \alpha_k = \langle \xi^k \rangle_z \quad (\text{S18})$$

Here and in the following $\langle \dots \rangle_z = - \int_{-z}^{\infty} d\xi (\dots) \frac{df_\xi^0}{d\xi}$, $f_\xi^0 = \frac{1}{1+e^\xi}$, and $z = \mu/T$.

With these definitions we first calculate r_1 . Using the equilibrium distribution Eq. (6) of the main text we find

$$r_1 = \frac{j_E}{j_c} = \frac{1}{e} (\mu + T \kappa), \quad \kappa = \frac{\langle \xi \sqrt{1 + \xi/z} \rangle_z}{\langle \sqrt{1 + \xi/z} \rangle_z} \quad (\text{S19})$$

To calculate r_2 we use that momentum conservation implies homogeneity of momentum-current in the steady

state. The latter can again be calculated with help of Eq. (6) given in the main text by expanding $T(x) = T + \delta T(x)$, $\mu(x) = \mu + \delta\mu(x)$ form small V . To linear order in V , i.e., for small δT and $\delta\mu$, we find

$$\text{const.} = j_p(x) = n\delta\mu(x) + n\kappa\delta T(x) + \text{const.}, \quad (\text{S20})$$

resulting in

$$r_2 = \frac{\partial_x \delta T}{\partial_x \delta \mu} = -\kappa^{-1} \quad (\text{S21})$$

To obtain r_3 we can directly use the definition of j_c^R and j_E^R given in the main text combined with the equilibrium distribution function (6) of the main text

$$\partial_x j_c^R = \frac{e\alpha_0}{h} \partial_x \delta\mu + \frac{e\alpha_1}{h} \partial_x \delta T \quad (\text{S22})$$

and

$$\partial_x j_E^R = \frac{\mu}{e} \partial_x j_c^R + \frac{T}{h} (\alpha_1 \partial_x \delta\mu + \alpha_2 \partial_x \delta T). \quad (\text{S23})$$

For the ratio r_2 we therefore obtain

$$r_3 = \frac{\partial_x j_E^R}{\partial_x j_c^R} = \frac{\mu}{e} + \frac{T}{e} \frac{\alpha_1 \kappa - \alpha_2}{\alpha_0 \kappa - \alpha_1} \quad (\text{S24})$$

Inserting above expressions into (S17) and solving for j_c gives Eq. (13) of the main text.

Measuring voltage profiles

To measure the voltage drop across a quantum wire one can, for example, use a weakly coupled tunneling contact realized by the tip of a scanning tunneling microscope. Assuming a constant tunneling matrix element M and a constant density of states ν_0 of the tunneling tip, the charge current $I_c(x)$ and the energy current $I_E(x)$ through the tip located at position x are given by

$$I_c(x) = \frac{4\pi e\nu_0}{h} |M|^2 \int dp (f_{x,p} - f_p^{\text{tip}}(\tilde{\mu}, \tilde{T})) \quad (\text{S25})$$

$$I_E(x) = \frac{4\pi e\nu_0}{h} |M|^2 \int dp \epsilon_p (f_{x,p} - f_p^{\text{tip}}(\tilde{\mu}, \tilde{T}))$$

Here $f_{x,p}$ is the distribution function of the wire and $f_{x,p}^{\text{tip}} = f_p^{\text{tip}}(\tilde{\mu}(x), \tilde{T}(x))$ is the Fermi distribution describing the occupation of the states in the tip. The latter is parametrized by the chemical potential $\tilde{\mu}$ and the temperature \tilde{T} .

The local chemical potential $\mu(x)$ of the quantum wire and the local temperature $T(x)$ of the wire are now obtained from the condition that particle and energy currents flow only if there is a difference in the chemical potential and temperature. $T(x)$ and $\mu(x)$ are therefore obtained from the condition

$$T(x) = \tilde{T}, \quad \mu(x) = \tilde{\mu} \quad \text{for } I_c(x) = I_E(x) = 0 \quad (\text{S26})$$

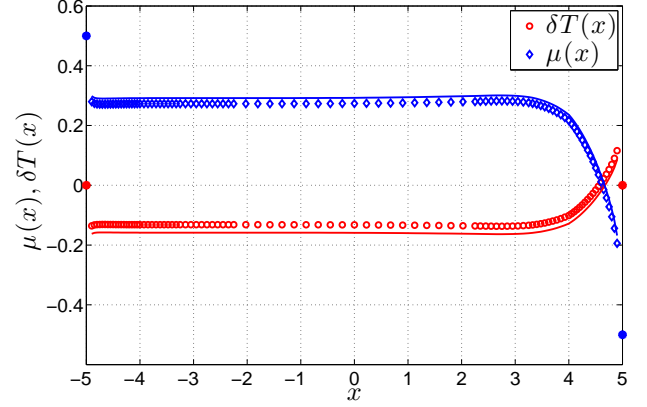


FIG. S4: Local chemical potential $\mu(x)$ (blue) and temperature $T(x) = T + \delta T(x)$ (red) (in units $|eV|$) for a wire of length $L = 10\ell_{\text{eq}}$ and voltage $eV/T = 0.4$. Symbols: Profiles obtained using Eq. (S25,S26), i.e. for voltage contacts in the tunneling regime. Solid lines: Corresponding profiles obtained from an alternative fitting procedure (used in the main text) defined by Eq. (S27). Both definitions give similar results for the parameters used in the paper.

Note that this definition can be used for distribution functions far from equilibrium (and the usual result is obtained in equilibrium). Eq. (S25) implies that the local chemical potential and temperature can directly be obtained from the local charge- and energy density of the system.

In Fig. S4 we show by the symbols chemical potential and temperature profiles obtained from the definition (S25,S26) for a wire of length $L = 10\ell_{\text{eq}}$ with $eV/T = 0.4$ at the QCP ($\mu = 0$). The separate points at $\pm L/2$ denote the chemical potential in the two leads.

In the insets of Fig. 1 of the main text we also show $\mu(x)$ and $T(x)$ but in this case we use a *different* definition of these quantities, which is more appropriate to illustrate our analytical arguments. In the main text, we fit the local charge, energy *and* momentum densities to the equilibrium distribution given by Eq. (6) of the main text, which depends not only μ and T but also on the average velocity u . At each point x , we therefore define the three space-dependent functions $u(x)$, $\mu(x)$, and $T(x)$ by

$$\sum_p f_{x,p} = \sum_p f_p^{\text{eq}}(u, \mu, T) \quad (\text{S27})$$

$$\sum_p \epsilon_p f_{x,p} = \sum_p \epsilon_p f_p^{\text{eq}}(u, \mu, T)$$

$$\sum_p p f_{x,p} = \sum_p p f_p^{\text{eq}}(u, \mu, T)$$

The two definitions, (S25,S26) and (S27), are different, as for the tunneling tip momentum is not conserved and we fit in the first case to an equilibrium function f^{tip} which depends only on the chemical potential and the temperature but not on the velocity.

For the range of applied voltages discussed in this paper, however, both methods lead to nearly identical profiles. This is shown in Fig. S4, where temperature and chemical-potential profiles obtained from Eqs. (S25,S26) (symbols) are compared to the corresponding curves from Eq. (S27) (lines) which are also used in the main text.

In conclusion, we have discussed an experimental procedure which allows to measure the local chemical potential and local temperature by using tunneling contacts. While we used in the main text a different definition (the one needed for our analytic arguments), the resulting profiles are almost identical which guarantees that the voltage and temperature profiles shown in the main text can

be measured.



- [1] J. Rech, T. Micklitz, and K. A. Matveev, Phys. Rev. Lett. **102**, 116402 (2009).
- [2] T. Micklitz, J. Rech, and K. A. Matveev, Phys. Rev. B **81**, 115313 (2010).
- [3] V. V. Aristov, *Direct Methods for Solving the Boltzmann Equation and Study of Nonequilibrium Flows*, Kluwer (2001).